Effect of the Carbamoyl Group Attached to an Axial Ligand Portion of a Novel Bleomycin Model on a Dioxygen Activating Reaction

Kazuo SHINOZUKA, Masayuki ISHIKAWA, Takayuki ARAI, Junya KOHDA, and Hiroaki SAWAI*

Department of Chemistry, Faculty of Engineering, Gunma University, Kiryu 376–0052, Japan.
Received May 11, 1988; accepted June 17, 1988

A Fe complex of a novel bleomycin model compound bearing a diaminopropionamide (DAPA) moiety as the axial ligand and a long alkyl chain as the steric factor around the 6th coordination site promoted reversible redox reaction and exhibited high oxygen activating ability. Kinetic analysis of the redox reaction in the presence of dioxygen and a reducing agent revealed that the presence of the carbamoyl group on the DAPA moiety facilitates the oxygenation–activation process of the Fe(II) complex, and the reduction process of the resulting Fe(III) complex.

Key words bleomycin; diaminopropionamide; iron complex; axial ligand; redox reaction; kinetic analysis

Bleomycin (BLM) is a histidine-containing glycopeptide antitumor antibiotic agent which is clinically prescribed for certain tumors.[1] The Fe(II) complex of BLM activates molecular oxygen and produces a hydroxyl radical through a characteristic redox cycle, thereby inducing oxidative degradation of deoxyribonucleic acid (DNA).[2,3] A number of studies have been conducted to clarify the structure–activity relationship of the BLM–metal complex using model compounds which simplify the metal coordination site of BLM. Through these studies, the presence of the carbamoyl group on the diaminopropionamide (DAPA) portion of BLM was found to be essential for antitumor activity although the group is not involved in metal chelation.[4] Kimura *et al.* and Sugiyama *et al.* reported that the carbamoyl group on the DAPA portion is effective in lowering the pK_a value of the primary amine, thereby facilitating coordination of this amine to the chelated metal ion and oxygen activation at near neutral pH.[5] However, the detailed role of the carbamoyl group in the characteristic Fe–BLM redox cycle still remains to be fully clarified.

To gain further information on the role of the carbamoyl group in the redox reaction, we conducted a study of novel BLM model compound (**II**) which has a DAPA moiety as the axial ligand, as well as a lauryl group as the steric factor in place of the disaccharide moiety of BLM around the sixth coordination site. The introduction of the latter group into a simplified BLM model compound (model compound **I** in Chart 1) was previously shown to enhance the stability of the chelated Fe(II) ion towards possible attack by OH^- ion during the redox reaction.[6] Herein, we wish to report the synthesis of **II** and the results of a kinetic study of the **II**–Fe complex showing for the first time that the carbamoyl group is responsible for facilitating the oxygenation–activation process of the Fe(II) complex and the reduction process of the resulting Fe(III) complex.

Results and Discussion

Preparation of the novel BLM model compound **II** was carried out as follows. The formyl pyridine derivative (**1**) was treated with Boc-protected diaminopropionamide derivative (Boc-DAPA) (**2**) in acetonitrile in the presence of molecular sieves (4A).[7] The resulting Schiff-base was reduced with $NaBH_4$, without isolation, to give **3**.[5a,7] Protection of **3** with the Z-group, and partial hydrolysis with LiOH gave **4**.[5a,8] Condensation of **4** with L-histidine derivative (**5**)[6] by the action of diphenylphosphoryl azide afforded the protected model compound (**6**). Treatment of **6** with a mixture of trifluoroacetic acid (TFA)·thioanisole·*m*-cresol[9] afforded model compound **II**. This synthesis is summarized in Chart 1. The synthesis of the corresponding model compound **I** which has a simple ethylenediamine moiety as the axial ligand was reported previously.[6]

The formation and coordination chemistry of **I**– and **II**–divalent metal complexes were studied by photometric methods. Tris–HCl buffer (20 mM, pH 7.2) containing 5% of methanol was used in the study to avoid possible micelle formation from **I** and **II**.[6] With the Cu(II) ion, both model compounds formed the corresponding Cu(II) complexes and displayed characteristic UV-*Vis* spectra with λ_{max} values close to that of the BLM–Cu(II) complex.[10,11] These results suggest that under these conditions, the model compounds are able to form Cu(II) complexes resembling the pyramidal type structure of the corresponding BLM–Cu(II) complex.

The compounds also form stable Fe(II) complexes in the presence of an Fe(II) ion and a nitrogen atmosphere with a λ_{max} value at 467 nm for both complexes.[10,11] In the presence of atmospheric dioxygen, the λ_{max} value shifted to around 390 nm due to formation of the Fe(III) complexes.[10,11] Addition of the reducing agent dithiothreitol (DTT) to the above samples gave a characteristic transient spectra with a λ_{max} value of about 630 nm, and then regenerated the spectra of the starting Fe(II) complex. The spectral changes brought about by the addition of DTT are due to the formation of the DTT–Fe(III) adduct and the subsequent reduction of the Fe ion. A further investigation using the electron paramagnetic resonance (EPR) method confirmed this redox reaction. Thus, the species in the presence of dioxygen exhibited a EPR spectrum of a typical low-spin Fe(III) complex with EPR parameters close to those of the BLM–Fe(III) complex.[12] On the other hand, the species in the presence of N_2 or DTT was EPR silent since the chelated Fe ion is in the spin-paired Fe(II) state.

The activation of O_2 and the generation of a hydroxyl radical by the reaction of **I**– and **II**–Fe(II) complexes with dioxygen was also studied by a EPR-spin trapping experiment using *N-tert*-butyl-α-phenyl nitron (BPN) as a spin-trapping

* To whom correspondence should be addressed.

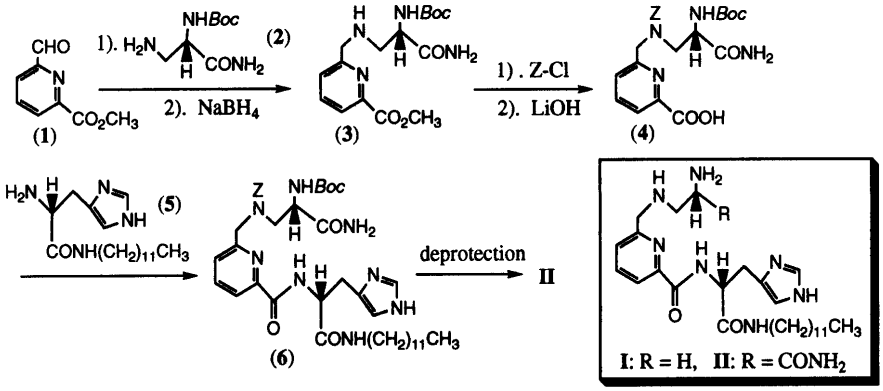

Chart 1. Synthesis and Structures of BLM Model Compounds

I- or II-Fe(II) + O_2 —(*koxiadd*, step 1)→ I or II-Fe(II)-O_2 —(*koxi*, step 2)→ transient activated I- or II-Fe(III)

—(step 3)→ stable I- or II-Fe(III)

$$kt_1 + \ln(\lambda_1 - \lambda_1') = \ln\{(\lambda_0 - \lambda_\infty)[1 - \exp(-k\Delta)]\} \quad (1)$$

Chart 2

Eq. 1. λ, absorbance of the reaction at t (s); $\lambda_{1'}$, absorbance of the reaction at $t+\Delta$ (s); λ_0, initial absorbance of the reaction (at $t=0$ s); λ_∞, absorbance of the reaction at $t=\infty$; Δ, an interval (s) for the measurement of absorbance.

I- or II-Fe(III) + DTT —(*kadd*)→ I or II-Fe(III)-DTT —(*kred*)→ I- or II-Fe(II)

$$\frac{1}{a-b}\ln\frac{b(a-x)}{a(b-x)} = kadd\ t \quad (2)$$

$$kred\ t_1 + \ln(\lambda_1 - \lambda_1') = \ln\{(\lambda_0 - \lambda_\infty)[1 - \exp(-kred\Delta)]\} \quad (3)$$

Chart 3

Eq. 2. a, initial concentration of the complex; b, initial concentration of DTT; x, concentration of the complex–DTT adduct after t (s); t, time (s).
Eq. 3. λ, absorbance of the reaction at t (s); $\lambda_{1'}$, absorbance of the reaction at $t+\Delta$ (s); λ_0, initial absorbance of the reaction (at $t=0$ s); λ_∞, absorbance of the reaction at $t=\infty$; Δ, an interval (s) for the measurement of absorbance.

agent. The obtained EPR spectra of the BPN–spin adduct (g=2.0, α^N=16.0 G) indicate that the hydroxyl radical was generated in the reaction. The O_2 activating ability of **I**– and **II**–Fe(II) complexes were 58%[6] and 90%, respectively, of that of the BLM standard. The latter value is higher than any other values observed for model complexes we have so far reported.[6,13,14] Thus, the O_2 activating ability of the **II**–Fe complex bearing a DAPA moiety is greatly enhanced compared to that of the **I**–Fe complex and the results are in accordance with the previous report.[5b] The observed difference in the O_2 activating ability between the **I**– and **II**–Fe complexes apparently arises from the presence of the carbamoyl group in model compound **II**. For quantitative analysis of the effect of the carbamoyl group, we have carried out a kinetic study on the rate of the redox reaction of the Fe(II) complexes with molecular oxygen and DTT by the UV-*Vis* method.

The reaction of the Fe(II) complexes of BLM model compounds with dioxygen took place within a second at 20 °C to form the corresponding Fe(III) complexes. The reaction is considered to proceed through the following pathway from the Fe(II) complex: 1) formation of an oxygenated intermediate, 2) activation of this oxygenated intermediate to the transient activated Fe(III) complex, and 3) conversion of the activated Fe(III) complex to the stable Fe(III) complex as shown in Chart 2.[15] Although the electronic spectrum of the transient activated species was very close to that of the stable Fe(III) species, and we could not differentiate them by the spectrophotometric method, the transient activated species was detected in small amounts along with the stable Fe(III) species by EPR 5 s after mixing of the Fe(II) complex with O_2 at 20 °C and subsequent freezing at 77 K. However, only the stable Fe(III) species was observed at 20 s after mixing. Thus, we have studied the reaction kinetics of oxygenation of the Fe(II) complexes and subsequent formation of Fe(III) species, by a stopped–flow apparatus, monitoring absorption change at 390 nm and at 20 °C. Step 1) reaction was carried out in the presence of an excess amount of O_2 (5, 10, 15, 20 ex.) over the Fe(II) complexes which is therefore considered to be a pseudo first-order reaction.[16] Under these conditions, the plots of log of absorption change against time at the initial stage (50—200 ms) are linear, indicating a first-order dependence of the reaction rate on the Fe(II) complex concentration. The pseudo first-order rate constants (k) of the reaction were determined by Guggenheim equation (Chart 2, Eq. 1). Plots of the pseudo first-order rate constants against O_2 concentration were also linear, as shown in Fig. 1.[16] Thus, reaction step 1) is second-order and the rate constants (k_{oxiadd}) determined from the slopes were 1.2×10^3 M^{-1} s^{-1} for

I–Fe and $5.4\times10^{3}\,M^{-1}s^{-1}$ for **II**–Fe. In reaction step 2), the oxygenated Fe(II) complex was converted to the Fe(III) species, independent of the oxygen concentration and, therefore, reaction step 2) is first-order (data not shown). The first-order rate constants (k_{oxi}) were $3.3\times10^{-1}\,s^{-1}$ for **I**–Fe and $2.7\,s^{-1}$ for **II**–Fe. The intermediate Fe(III) species subsequently converted to the stable Fe(III) species, although these two are spectrophotometrically indistinguishable. The rate constants (k_{oxiadd} and k_{oxi}) thus obtained were both several times greater for the **II**–Fe complex compared to **I**–Fe.

Next, reaction of the **I**– and **II**–Fe(III) complexes with DTT was performed at 25 °C under second-order conditions, and the rates of reaction were determined by monitoring the absorbance at 630 nm, which corresponds to that of the **I**– and **II**–Fe(III)–DTT adduct. The reaction is assumed to proceed through two successive steps, namely, the formation of the **I**– or **II**–Fe(III)–DTT adduct and the subsequent reduction of the Fe ion to regenerate **I**– or **II**–Fe(II) complexes as shown in Chart 3. From the Chart, the second-order rate constant (k_{add}) and the first-order rate constant (k_{red}) are expressed by Eqs. 2 and 3, respectively.

Figure 2-a shows the second-order plots of the first reaction. The second-order rate constants for the model complexes were determined from the slopes and are almost the same ($k_{add}=1.01\,M^{-1}s^{-1}$ for **I**–Fe and $1.19\,M^{-1}s^{-1}$ for **II**–Fe). Figure 2-b shows the first-order plots (Guggenheim plots) of the second reaction. Again, the first-order rate constants were determined from the slopes. In this case, however, the rate constant of complex **II** is greater than that of **I** ($k_{red}=9.82\times10^{-2}\,s^{-1}$ for **I**–Fe, and $1.51\times10^{-1}\,s^{-1}$ for **II**–Fe). These results clearly indicate that the presence of the carbamoyl group promotes the reduction of the oxidized Fe ion while it has little effect on the coordination of the reducing agent. The promotion of the reduction is presumably due to the electron–withdrawing effect of the carbamoyl group which facilitates the transfer of an electron from the reducing agent to the Fe ion. These results indicate that the presence of the carbamoyl group in BLM accelerates the redox cycle, making possible a higher turn-over compared to that without this group.

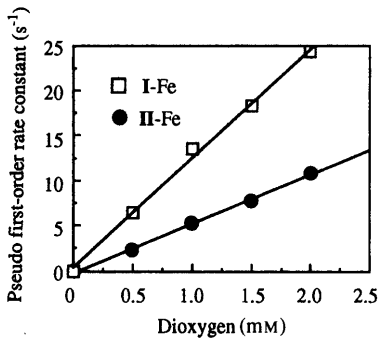

Fig. 1. Second-Order Plots (Pseudo First-Order Rate Constants *vs.* Dioxygen Concentration) for the Reaction of **I**– and **II**–Fe(II) with Dioxygen (Step 1).

In conclusion, we have demonstrated for the first time the role of the carbamoyl group in the rate of redox reaction. Thus the presence of this group facilitates both the oxygenation-activation process of the Fe(II) complex and the reduction process of the resulting Fe(III) complex by the reducing agent, yielding an enhancement of the oxygen activating ability of the Fe complex.

Experimental

^{1}H-NMR spectra were measured with a Varian Gemini-200 spectrometer and chemical shifts are given in δ (ppm) with tetramethylsilane as internal standard. UV-visible spectra were measured with a Hitachi U-3200 spectrophotometer. EPR-spectra were measured with a JEOL JES-RE2X spectrophotometer. Optical rotation was determined with a JASCO DIP-1000 using methanol as solvent. All organic solvents for reactions were dried and distilled before use, in the usual way.

N^{α}-[6-[[*N*-[(2*S*)-2-[Carbamoyl-2-(*tert*-butoxycarbonyl)amino]ethyl]-*N*-(benzyloxycarbonyl)-amino]methyl]pyridine-2-carbonyl]-L-histidine laurylamide (**6**).

Compound (**3**)[5a,7] (402 mg, 1.14 mmol) was dissolved in a mixure of CH_2Cl_2 (12 ml) and 0.2 M–NaOH (9 ml). To this mixture was added a solution of benzyloxycarbonyl chloride (1.71 mmol) in CH_2Cl_2 (10 ml) dropwise under vigorous stiring. The reaction was then stirred at room temperature for 3 h, and extracted with CH_2Cl_2 (30 ml×4). The isolated organic layer was dried over $MgSO_4$ and evaporated to give an oil. The oil was purified by silica gel chromatography (eluent, CH_2Cl_2/MeOH 19 : 1). Evaporation of the appropriate fractions gave a Z-protected form of **3** as a white solid (457 mg, 82.4%). The foregoing compound (321 mg, 0.66 mmol) was dissolved in tetrahydrofuran (THF), (5.4 ml). To this solution was added 0.1 M LiOH (18 ml) and the mixture stirred for 1.5 h with cooling in an ice-bath. After removal of THF under reduced pressure, the pH of the remaining solution was adjusted to 3 to 4 with aqueous citric acid, followed by extraction with dichloromethane (50 ml×6). The separated organic portion was dried over $MgSO_4$ and evaporated under reduced pressure to give compound (**4**)[5a,8] as a colorless oil, which was used in the next step without further purification. Compounds (**4** and **5**)[6] were dissolved in dry *N*,*N*-dimethylformamide (DMF) (5 ml) and the mixture was cooled in an ice-bath. To this solution was added a solution of diphenylphosphoryl azide (DPPA) (0.14 ml, 0.80 mmol) in dry DMF (2.7 ml). After stirring at 0 °C for 20 min, Et_3N (0.11 ml, 0.80 mmol) in dry DMF (3 ml) was added at 0 °C and the mixture stirred at 0 °C for 3 h, and at room temperature for 2 d. Ethyl acetate (200 ml) was added to the mixture, and the mixture washed with 5%-aqueous $NaHCO_3$ (20 ml×2), distilled water (20 ml×2) and saturated brine. After drying over $MgSO_4$, the organic portion was concentrated under reduced pressure and the residue purified by silica gel chromatography (eluent, CH_2Cl_2/MeOH/conc.NH_4OH 9 : 1 : 0.1) to give **6** (416 mg, 80.3%). ^{1}H-NMR ($CDCl_3$) δ: 0.85 [m, 3H, CH_3 of $(CH_2)_{11}CH_3$], 1.21 [m, 18H, $(CH_2)_9$ of $(CH_2)_{11}CH_3$], 1.36 [s, 9H, $C(CH_3)_3$], 1.37—1.52 [m, 2H, CH_2 of

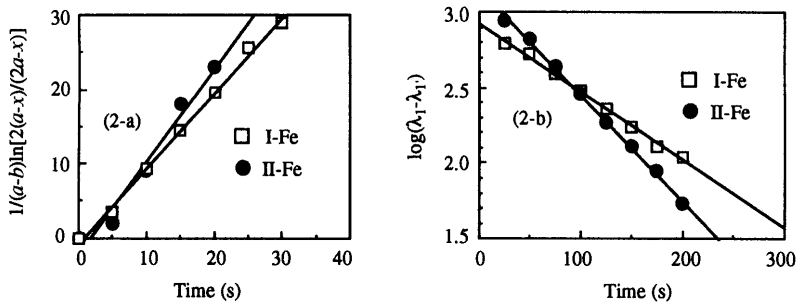

Fig. 2. Second-Order Plots for the Reaction of **I**– and **II**–Fe(III) with DTT (2-a, Right) where $b=2a$, and First-Order Plots (Guggenheim Plots) for the Regeneration of **I**– and **II**–Fe(II) (2-b, Left)

$(CH_2)_{11}CH_3$], 3.08—3.15 (m, 1H, $C_\beta H$ of β-Ala), 3.05—3.20 [m, 2H, CH_2 of $(CH_2)_{11}CH_3$], 3.25—3.35 (m, 1H, $C_\beta H$ of β-Ala), 3.63—3.83 (2H, m, $C_\alpha H_2$ of His), 4.47—4.75 (m, 3H, $C_\alpha H$ of β-Ala and $PyCH_2$), 4.91 (s, 1H, $C_\beta H$ of His), 5.14 (s, 2H, $PhCH_2$), 7.01 [s, 1H, Im (5)], 7.17—7.27 (m, 5H, each Ph), 7.27 [d, 1H, J=7.6 Hz, Py (5)], 7.34 (s, 1H, Im (3)], 7.66 [t, 1H, J=7.6 Hz, Py (4)], 8.00 [d, 1H, J=7.6 Hz, Py (3)]; IR (KBr): 3340 m (br), 2925 m, 2855 m, 1685 m, 1520 m, 1456 m, cm^{-1}.

N^α-[6-[[*N*-[(2*S*)-2-Amino-2-carbamoylethyl]amino]methyl]pyridine-2-carbonyl]-L-histidine laurylamide (**II**).

The foregoing compound was dissolved in a mixture of TFA (18 ml), thioanisole (1.8 ml) and *m*-cresol (1.8 ml) and the mixture stirred at room temperature for 72 h. Volatile materials were removed by evaporation and the residual oil added dropwise to vigorously stirred ether. The resulting precipitate was collected by filtration, washed with ether and purified by silica gel chromatography (eluent, CH_2Cl_2/MeOH/conc.NH_4OH 5 : 1 : 0.1) to give **II** as a white powder (170 mg, 87.2% from (**3**)), mp 125.4—126.0 °C. ^{1}H-NMR (CD_3OD) δ: 0.74—0.82 [m, 3H, CH_3 of $(CH_2)_{11}CH_3$], 1.13—1.29 [m, 18H, $(CH_2)_9$ of $(CH_2)_{11}CH_3$], 1.30—1.40 [m, 2H, CH_2 of $(CH_2)_{11}CH_3$], 2.68—2.78 (m, 1H, $C_\beta H$ of β-Ala), 2.83—2.91 (m, 1H, $C_\beta H$ of β-Ala), 3.01—3.17 [m, 4H, CH_2 of $(CH_2)_{11}CH_3$ and $C_\alpha H_2$ of His], 3.26 (s, 2H, $PyCH_2$), 3.45—3.54 (m, 1H, $C_\alpha H$ of β-Ala), 4.67 (s, 1H, $C_\beta H$ of His), 6.80 [s, 1H, Im (5)], 7.32 [d, 1H, J=7.5 Hz, Py (5)], 7.44 (s, 1H, Im (3)], 7.74 [t, 1H, J=7.5 Hz, Py (4)], 7.80 [d, 1H, J=7.5 Hz, Py (3)]. FAB-MS *m/z*: 543 (M^+). $[\alpha]_D^{25}$=+6.45° (*c*=5.0% in MeOH). *Anal.* Calcd for $C_{28}H_{46}N_8O_3 \cdot 1/2H_2O$: C, 60.95; H, 8.59; N, 20.3. Found: C, 60.76; H, 8.27; N, 20.1.

Kinetic Studies of Reduction of the Fe(III) Model Complex with DTT Stopped-flow kinetic measurement of the oxygenation of the Fe(II)-complex was made after rapid mixing of equal volumes of solutions of the Fe(II) BLM-model complex and 0—2.0 mM oxygen. The later solutions were prepared by the published procedure.[16] All solutions used in the experiments were purged of oxygen by swirling them for 2 h under a stream of N_2. A solution of Fe(II) complex (0.10 mM) in 10 mM Tris–HCl buffer containing 5% methanol was prepared by mixing an oxygen-free solution of iron(II) sulfate (0.10 mM) in water with oxygen-free solutions containing 1.5 mol equivalents of the model compound, and pH was adjusted to 7.2 by adding 1.0 M Tris–HCl (pH 7.2). Kinetic measurements were carried out using an Otsuka Electronics RA401 stopped-flow apparatus at 20 °C. The reaction of the Fe(II) complex with O_2 was monitored at the λ_{max} of the Fe(III) complex, 390 nm. The first, rapid process was analyzed by the spectral change between 50—200 ms after mixing, and the second, slow process, between 400—2100 ms when 2.0 mM–O_2 was used. The pseudo-first order rate constant (k) was determined from the Guggenheim equation (Eq. 1). A linear relationship was obtained from plots of pseudo first-order rate constants against O_2 concentration and the rate constant of the first step (k_{oxiadd}) was determined from the slope. The second kinetic event was first-order with respect to the first accumulated product and independent of oxygen concentration, therefore, the rate constant of the second step (k_{oxi}) coincides with the first-order rate constant.

Reduction of the Fe(III) complex with DTT was monitored by UV-visible spectral change using a Hitachi UV 3200 double-beam spectrophotometer at 25 °C. The rates of the reactions were determined by monitoring the absorbance at 630 nm which corresponds to the absorbance of the DTT adduct of the Fe(III) complex. The DTT–Fe(III) complex (0.5 mM) was prepared by addition of 2.0 mol equivalents of DTT (aqueous solution) to the Fe(III)–BLM model complex in 50 mM Tris–HCl buffer (pH 7.2) containing 5% of methanol. The first step is the second-order reaction, and the rate constant (k_{add}) was determined by Eq. 2. The rate constant of the second reaction (k_{red}) was determined by the Guggenheim plot (Eq. 3).

References and Notes

1) Carter S. K., "Bleomycin: Current Status and New Developments," Academic Press Inc., New York, 1978, pp. 9—14.
2) *a*) Kane S. A., Hecht S. M., "Progress in Nucleic Acid Research and Molecular Biology," Academic Press Inc, New York, **49**, 313—352 (1994); *b*) Ohno M., Otsuka M., "Recent Progress in the Chemical Synthesis of Antibiotics," ed. by Lukacs G., Ohno M., Spring-Verlag, New York, 1990, pp. 387—414.
3) Sausville E. A., Stein R. W., Peisach J., Horwitz S. B., *Biochemistry*, **17**, 2746—2754 (1978).
4) Sugiura Y., *J. Am. Chem. Soc.*, **102**, 5208—5215 (1980).
5) *a*) Kimura E., Kurosaki H., Kurogi Y., Shionoya M., Shiro M., *Inorg. Chem.*, **31**, 4313—4321 (1992); *b*) Sugiyama T., Ohno M., Shibasaki M., Otsuka M., Sugiura Y., Kobayashi S., Maeda K., *Heterocycles*, **37**, 275—282 (1994).
6) Shinozuka K., Morishita H., Yamazaki T., Sawai H., *Tetrahedron Lett.*, **32**, 6869—6872 (1991).
7) Otsuka M., Yoshida M., Kobayashi S., Ohno M., Sugiura Y., Takita T., Umezawa H., *J. Am. Chem. Soc.*, **103**, 6986—6988 (1981).
8) Umezawa H., Takita T., Sugiura Y., Otsuka M., Kobayashi S., Ohno M., *Tetrahedron*, **40**, 501—509 (1984).
9) Takeyama M., Koyama K., Inoue K., Adachi H., Tobe T., Yazima H., *Chem. Pharm. Bull.*, **28**, 1873—1883 (1980).
10) The following λmax values were obtained; 602 nm for I–Cu(II), 595 nm for II–Cu(II), 596 nm for BLM–Cu(II),[11] 476 nm for BLM–Fe(II),[11] and 385 nm for BLM–Fe(II)+O_2.[11]
11) Sugiura Y., Suzuki T., Otsuka M., Kobayashi S., Ohno M., Takita T., Umezawa H., *J. Biol. Chem.*, **258**, 1328—1336 (1983).
12) The following EPR signals were obtained; gx=2.345, gy=2.179, gz=1.887 for I–Fe(III); gx=2.332, gy=2.178, gz=1.890 for II–Fe(III); gx=2.431, gy=2.185, gz=1.893 for BLM–Fe(III).[4]
13) Kohda J., Shinozuka K., Sawai H., *Tetrahedron Lett.*, **36**, 5575—5578 (1995).
14) Arai T., Shinozuka K., Sawai H., accepted for publication in *Bull. Chem. Soc. Japan.*
15) *a*) Burger R. M., Peisach J., Horwitz S. B., *J. Biol. Chem.*, **256**, 11636—11644 (1981); *b*) Burger R. M., Kent T. A., Horwitz S. B., Munck E., Peisach J., *J. Biol. Chem.*, **258**, 1559—1564 (1983).
16) Burger R. M., Horwitz S. B., Peisach J., Wittenberg J. B., *J. Biol. Chem.*, **254**, 12299—12302 (1979).